Growing lithium tetraborate crystals in the YXl/53° and XZb/45° directions and their characteristics

A. Gotalskaya, A. Kharitonov, V. Stassevich, V. Bezdelkin

JOURNAL DE PHYSIQUE IV
Colloque C2, supplément au Journal de Physique III, Volume 4, février 1994

Growing lithium tetraborate crystals in the YXl/53° and XZb/45° directions and their characteristics

A.N. GOTALSKAYA, A.V. KHARITONOV, V.N. STASSEVICH and V.V. BEZDELKIN

Scientific Research Institute "FONON", 105023 Moscow, Krasnobogatyrskaya 44, Russia

Different methods of charge synthesization are discussed. Peculiarities of growing LBO crystal in the YXl/53° and XZb/45° directions by Czokhralsky method are given. Morphology of LBO crystals is described. Characteristics of LBO-resonators are given.

Lithium tetraborate ($Li_2B_4O_7$), LBO, is a promising material for application in electronics, which attracts attention in connection with a possible application in piezoelectric SAW and BAW products [1,2]. Lithium tetraborate is also a non-linear optical material, a super-ion conductor [3]. It can be applied in photoelectric sensors in the IR region and in radiation dosimeters [4].

For manufacturing SAW and BAW devices the plates of zero cuts YXl/53° and XZb/45°, respectively, have been used. We have investigated initially LBO crystal grown by Czokhralsky method in the directions [001] and [110] and growth and charge synthesis processes.

The quality of industrial LBO charge being concentrated by lithium containing compounds, we tried different methods of charge synthetization: in solutions and by solid phase- and liquid phase reaction methods.

When obtaining LBO charge in solutions the following reagents have been used: $Li_2CO_3+H_3BO_3$, $LiOH+H_3BO_3$. In the first case we have tried to obtain LBO via an intermediate composition $Li_2O \cdot 2B_2O_3 \cdot 3H_2O$ by maintaining constant pH of the solution. This is, however, a sufficiently labour-consumpting technology, although it allows to

maintain exactly a stoichiometric composition. We have also attempted to obtain LBO pure charge by hydrothermal method by using reagents LiOH and H_3BO_3. A single crystalline phase $Li_2B_4O_7$ (with gram size 1-2 cm) has been obtained at t_{med}=450°C in platinum lined autoclaves of V=0,4 l but the yield of charge was rather low.

The method of LBO charge obtained by solid state reaction method is a more technological one, however, it was difficult to obtain exactly the stoichiometric composition. The process of growth was a multistage one: annealing at 90°C during 40 h under constant mixing, synthesis at 550°C during 6 h, annealing during 4 h at 800°C in vacuum of 10^{-3}mm Hg for water traces and CO_2 removal. The synthesis results were controlled by DTG-method.

The method of liquid phase reaction in the melt proposed by other authors [5] was also investigated. First, the platinum crucible was glued, then a calculated quantity of boron oxide was melted. The crucible was weighted after cooling and then a calculated quantity of lithium carbonate was added at 1000°C. The crucible was weighted again and the composition corrected. In the two last cases high quality crystals were obtained. Good results were also obtained when employing double recrystallization and addition of boron oxide in small quantity for correcting stoichiometric composition, because during the crystal growth a separation of an easy volatile phase $Li_2B_8O_{13}$ can occur.

Morphological investigation of the boules grown in the [001] and [110] directions was then carried out. During LBO boules examination grown along the Z-axis one can easily note characteristic steps of degenerate faces at their external surfaces, which are located at angles of 45° to each other (fig.1).

The largest rough steps of degenerate faces with the height of 0.6-1.2 mm are located at angles of 90° to each other. The smaller steps define the crystallographic direction [100]/[010] - the X (Y)-axis, the large ones correspond to the [110] - direction. LBO boules grown on [110] seeds are characterized by four well distinguishable plain steps of degenerate faces with the height of 0.1-0.3 min located at angles of 90°.

One pair of these faces corresponds to the [001] direction. Besides the main faces, weekly distinguishable faces can be observed additionally at the conical part of the crystal. These faces made an angle of 37° to the [001] faces and correspond, possibly, to the exit

points of the normal to atomic plane [112] ($ZZ'=52^{o}30'$). An interesting feature of LBO boules, grown at [110] seeds is clearly visible inclined smooth faces in the upper part of the boule near to growing seed, which are located at an angle of $52^{o}20'$ in the direction of the Z-axis. Indentification of these inclined faces by means of atomic plane with the diffraction indices [448] confirmed their crystallographic orientation [112] ($XC=45^{o}$, $ZZ'=52^{o}30'$).

As result of X-ray investigations a table of experimental angular parameter values and relative intensities of atomic plane reflection of LBO crystals was specified for practical applications (table 1).

More exact definition of LBO elementary cell parameters was made by using three reflection pairs from atomic planes with large angle values $\theta_{hkl} \rightarrow 90^{o}$; $a=9,4772$ Å , $c=10,2876$ Å. Comparison of these values with the initially accepted data confirms their satisfactory coincidence with the measuring error of 0,007 A for "a" and with 0,015 Å error for "c". Taking into account considerable influence of charge purity and growth conditions on elementary cell parameter values such difference can be admitted.

For these directions an optimum LBO crystal cutting technology into sections has been developed (fig.2, 3). However during the cutting process considerable rejects have been obtained. Therefore, we have grown LBO crystals in the directions $YX1/53^{o}$ and $XZb/45^{o}$ with the diameter of 40 mm and the length of 50 mm in platinum crucibles in an oxidating atmosphere for evaporation suppression of easy volatile borates in installations "Crystal" with an induction heating of a crucible (fig.4).

During LBO single crystal growth, the investigators come across a number of difficulties:

1. The charge quality for this material is of prime importance, because the melt has a very visc ous glassy texture, the exit of gaseous components at the surface being rather difficult from it. In addition to this, with temperature fluctuations near the surface of the melt, the solubility of gaseous components in the surface layer occurs. As the result, the gaseous components come into the melt. Then by means of convection currents they are trapped by growing crystal and figure in the "as grown" crystal as growth column and facettes (figure 5).

2. With crystals having a low melting point, the heat dissipation

occurs at the expense of heat transfer to the grown crystal. It is therefore difficult to exclude heat energy dissipitation with small heat transfer and low melting temperature.

3. LBO crystals have a strong anisotropy of linear thermal expansion coefficients along different crystallographic directions. Therefore in the process of LBO growth stresses occur, cracks and anomalous edges at the crystal surface can appear. Thus, for successful LBO crystal growing it is necessary to create "soft" growth conditions.

Based on peculiarities of LBO crystals we have developed a heat assembly with upper resistive heating enabling to set up minimum axial temperature gradients near the crystallization front. This makes it possible to decrease stresses in crystals, to lower temperature fluctuations influence on gaseous impurity entering the crystal. All this enables to maintain stable temperature conditions for the LBO crystal growth of 40 mm in diameter without facetted regions. The technological growth parameters are also of great importance for LBO crystals. For ensuring "soft" growth conditions, it is necessary to maintain low rotation rates (2-4 rot/min) and low growth rates (0.1-0.4 mm/h).

In order to decrease viscosity of the melt we increased melting temperature, by adding 0.1-0.2 mass per cent of lantanium oxide, which enables us to decrease gaseous inclusions in crystals. This additive does not influence piezoelectric properties of LBO crystals.

With small temperature gradients near the melt surface LBO crystals grow up equally well along the YX1/53° and XZb/45° crystallographic directions and have a well developed faces.

The main feature of LBO resonator technology is its solubility in liquid media. In this connection we were interested in obtaining more exact kinematic curves of LBO water and HNO_3 (60% concentration) dissolution at different temperatures (fig.6). LBO solution rate in deionized water with specific resistivity of 1 MOhm cm at temperatures of 55°C, 60°C and 100°C is equal to 0.02, 0.05 and 0.25 μm/min, respectively. LBO solution rate in 60% HNO_3 at temperatures of 19°C, 40°C and 60°C was 2.6, 4.2 and 30 μm/min. Reproducibility of solution rate depends on the sample surface state and the solution purity. Chemical etching of LBO plates after lapping was made in acid mixture taken in the proportion: HNO_3:HCL:H_2O = 1:1:1 at room temperature. The solubility rate in this solution is ~ 10 μm/min. The surface roughness

Table 1: Angle parametres of atomic planes of LBO crystal

$CuK_{\alpha 1,2}$ X-ray

Diffraction index of atomic plane hkl	Angle of trace x_{Chkl}	Angle between atomic plane hkl and axis Z ZZ'_{hkl}	Initial installation of angle sample φ'_{hkl}	Angle of Bragg θ_{hkl}	Double Angle of Bragg $2\theta_{hkl}$	Relative intensity of reflection, %
1	2	3	4	5	6	7
020	0°	0°00'00"	-3°57'30"	9°21'40"	18°43'20"	50
040	–"–	–"–	5°40'00"	18°59'10"	37°58'20"	40
060	–"–	–"–	15°51'20"	29°10'30"	58°21'00"	17
080	–"–	–"–	28°13'40"	40°32'50"	81°05'40"	7
0100	–"–	–"–	41°04'00"	54°23'10"	108°46'20"	3,5
082	–"–	12°58'10"	28°32'30"	41°51'40"	83°43'20"	0,8
062	–"–	17°04'10"	17°20'50"	30°40'00"	61°20'00"	2,0
042	–"–	24°43'50"	7°39'00"	20°58'10"	41°56'20"	12
084	–"–	–"–	32°24'00"	45°43'10"	91°26'20"	12
064	–"–	31°33'20"	21°35'00"	34°54'10"	69°48'20"	4,0
086	–"–	34°38'20"	38°53'50"	52°13'00"	104°26'00"	7
022	–"–	42°39'00"	-0°33'10"	12°46'00"	25°32'00"	9
044	–"–	–"–	12°54'30"	26°13'40"	52°27'20"	18
066	–"–	–"–	28°13'00"	41°32'10"	83°04'20"	10
088	–"–	–"–	48°49'40"	62°08'50"	124°17'40"	12
068	–"–	50°50'50"	39°15'20"	50°34'30"	101°09'00"	3,0
046	–"–	54°06'20"	20°21'20"	33°40'30"	67°21'00"	12
06.10	–"–	56°55'20"	50°01'10"	63°20'20"	126°40'40"	10
024	–"–	61°30'30"	6°36'00"	19°55'10"	39°50'20"	10
048	–"–	–"–	29°38'40"	42°58'50"	85°55'40"	6
04.10	–"–	66°31'40"	41°24'00"	54°43'10"	109°26'20"	4,2
026	–"–	70°06'30"	45°13'00"	28°32'10"	57°04'20"	9
04.12	–"–	–"–	59°34'00"	72°53'10"	145°46'20"	2,7
028	–"–	34°48'50"	25°02'30"	38°21'40"	76°43'20"	5
02.10	–"–	77°45'00"	36°42'00"	50°01'10"	100°02'20"	3,5
02.12	–"–	79°44'40"	52°38'00"	65°59'10"	131°54'20"	4,0
004	–"–	90°00'00"	4°05'50"	17°25'00"	34°50'00"	100
008	–"–	–"–	23°28'00"	36°47'40"	73°34'20"	5
00.12	–"–	–"–	50°39'20"	63°58'30"	127°57'00"	15
2.100	11°18'40"	0°00'00"	42°40'30"	55°59'40"	111°59'20"	7
2.102	–"–	10°14'30"	44°04'00"	57°23'10"	114°46'20"	45
2.104	–"–	19°52'00"	48°29'00"	61°48'10"	123°36'20"	6
2.106	–"–	28°27'20"	51°15'30"	70°34'40"	141°09'20"	12
280	14°02'10"	0°00'00"	28°45'20"	42°04'30"	84°09'00"	2,5
282	–"–	12°35'40"	30°02'30"	43°21'40"	86°43'20"	3,8
284	–"–	24°04'40"	33°54'00"	48°13'10"	94°26'20"	1,0
286	–"–	33°50'00"	40°28'00"	53°47'10"	107°34'20"	3,5
288	–"–	41°47'40"	50°42'00"	64°01'40"	128°02'20"	2,0
260	18°26'10"	0°00'00"	17°36'30"	30°55'40"	61°51'20"	25
262	–"–	16°14'30"	19°02'50"	32°22'00"	64°44'00"	4,0
264	–"–	30°13'30"	23°10'50"	36°30'00"	73°00'00"	22
266	–"–	41°09'00"	29°43'30"	43°02'40"	86°05'20"	0,5
268	–"–	49°21'50"	33°48'00"	52°07'10"	104°14'20"	5
2610	–"–	55°31'40"	51°58'00"	65°17'10"	130°34'20"	3,5
4.100	21°48'10"	0°00'00"	47°46'20"	61°05'30"	122°11'00"	5
4.102	–"–	9°42'30"	49°18'50"	62°38'00"	125°16'00"	0,5
4.104	–"–	18°53'10"	54°23'00"	67°42'10"	135°24'20"	1,5
240	26°33'20"	0°00'00"	7°58'50"	21°18'10"	42°36'00"	30
480	–"–	–"–	33°18'30"	46°37'40"	93°15'20"	9
482	–"–	11°38'20"	34°36'00"	47°55'10"	95°50'20"	3,7
242	–"–	22°23'20"	9°48'50"	23°08'00"	46°16'00"	2,5
484	–"–	–"–	38°31'00"	51°30'10"	103°40'20"	2,7
486	–"–	31°42'50"	45°23'50"	58°43'00"	117°26'00"	1,0
244	–"–	39°29'10"	14°46'00"	28°05'10"	56°10'20"	5,5
246	–"–	51°01'20"	21°59'00"	35°18'10"	70°36'20"	1,0
248	–"–	58°44'50"	31°10'00"	41°29'10"	83°58'20"	1,2
24.10	–"–	64°06'20"	43°01'30"	56°20'40"	112°41'20"	1,5
24.12	–"–	67°58'20"	62°30'00"	76°49'10"	151°38'20"	0,7
6.100	30°57'50"	0°00'00"	58°07'20"	71°26'30"	142°53'00"	2,5
6.102	–"–	8°58'40"	60°22'00"	73°41'10"	147°22'20"	4,2
460	33°41'24"	0°00'00"	22°33'00"	35°52'10"	71°44'20"	8
462	–"–	14°19'20"	23°53'30"	37°12'40"	74°25'20"	2,0
464	–"–	27°04'00"	27°50'30"	41°09'40"	82°19'20"	2,7
466	–"–	37°28'10"	34°16'30"	47°35'40"	95°11'20"	0,5
468	–"–	45°37'20"	43°37'50"	56°57'00"	113°54'00"	1,2
46.10	–"–	51°56'40"	58°41'10"	72°00'20"	144°00'40"	0,7
682	36°52'10"	10°26'20"	42°25'20"	55°44'30"	111°29'00"	1,2
684	–"–	20°13'40"	46°43'00"	60°02'10"	120°04'20"	3,0
686	–"–	28°55'50"	54°56'00"	68°15'10"	136°30'20"	6
220	45°00'00"	0°00'00"	-0°01'00"	13°15'10"	26°36'20"	3,7
440	–"–	–"–	14°02'00"	27°21'10"	54°42'20"	1,2
660	–"–	–"–	30°16'40"	43°35'50"	87°11'40"	17
880	–"–	–"–	53°33'40"	66°52'50"	133°45'40"	8
884	–"–	18°02'20"	61°59'10"	75°18'20"	150°36'40"	15
664	–"–	23°28'20"	35°25'30"	48°45'00"	97°30'00"	22
444	–"–	33°04'40"	19°57'10"	33°16'20"	66°32'40"	6
668	–"–	40°58'30"	52°41'10"	66°00'20"	132°00'40"	28
224	–"–	52°29'20"	8°51'20"	22°10'30"	44°21'00"	100
448	–"–	–"–	35°43'00"	49°02'10"	98°04'20"	3,7
228	–"–	69°00'10"	26°35'20"	39°54'30"	79°49'00"	15
22.12	–"–	75°38'50"	54°44'30"	68°03'40"	136°07'20"	2,0

was not deteriorated in this case. LBO resonators fabricated with LBO piezoelectric elements in the form of flat wafers with 7 mm in diameter and thickness t~ 215 μm with silver electrodes of 3 mm in diameter had the following parameters (tabl 2). Dependences of temperature-frequency coefficient, electromechanical coupling factor of B- and C-modes in LBO on the angle of cut YXl/β of piezoelectrical element are given on fig 7 and 8.

Table 2. LBO resonator parameters

Frequency f MHz	Resonance spacing %	Quality factor Q	Frequency constant kHz mm	Capacitance parallel C_o, pF	Capacitance motional C_1, pF	Motional inductance L_1, H
7.55	2-2.2	$(3-5).10^3$	1645	3.69	0.143	0.0031

References

[1] Whatmore R.W., SHorrocks N.M., O'Hara C, Ainger F.W., Young I.M., "Lithium tetraborate: a new temperature-compensated SAW substrate material", J.Electronics letter, 17 (1981) 11-12.

[2] Emin C.D.J., Werner J.E., "The bulk acoustic wave properties of lithium tetraborate", 37th ASFC 1983 pp. 136-143

[3] Aliev A., Burak Ja., Lysejko U., "Electrophysical properties of new super-ion conductor", Izv. AN USSR, Nonorganic Materials, 26 (1990), 9, 18-20 (in russian)

[4] Burak Ja., Dovgiy Ja., "Optycal function of lithium tetraborate crystal J.Optics and spectroscopie, 69 (1990), 5, pp.1180-1182 (in russian)

[5] Nefeodov B.A., Balakireva T.P., Provotorov M.V., Mayer A.A., "Growth LBO single crystal of Czokhralsky method", 7th USSR Conference of Chemistry and Technology of rare elements", Apatitiu, 1988, 165-168 (in russian)

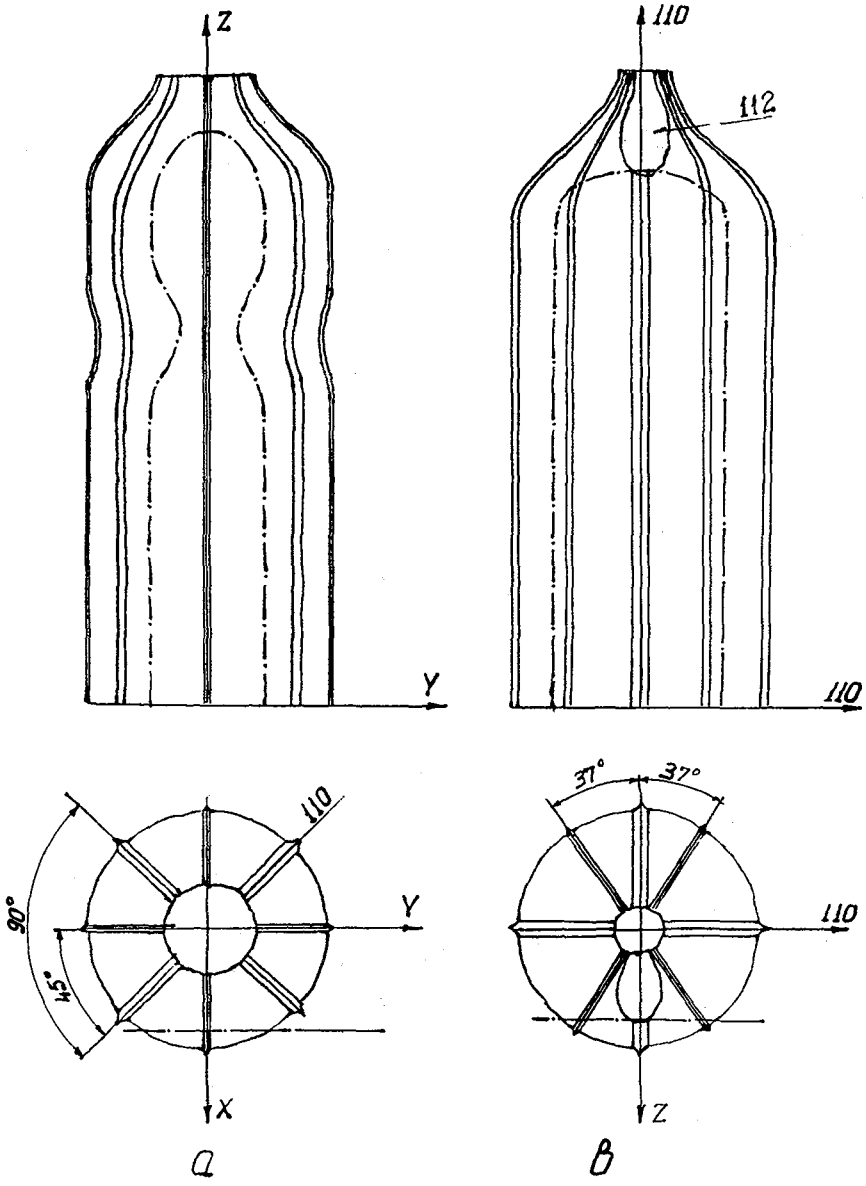

Fig. 1. LBO crystal morpfology

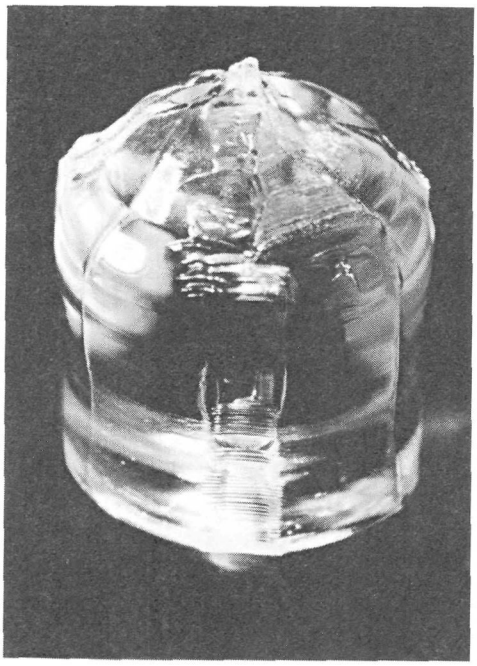

Fig. 2. "As grown" crystal LBO in the direction YX1/53°

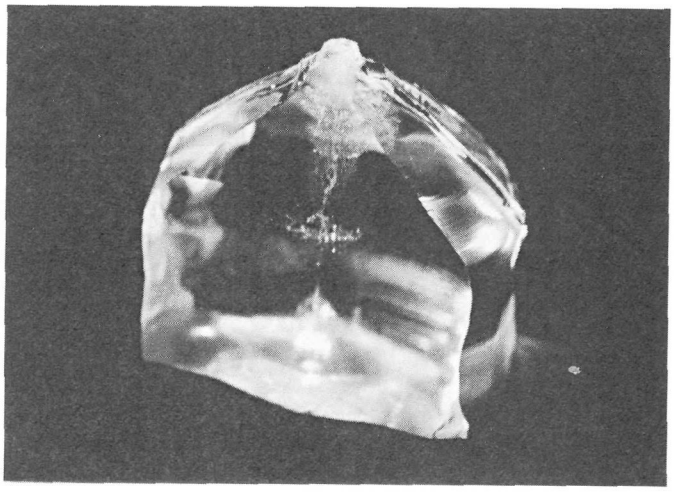

Fig. 3. A growth column and facets LBO crystal

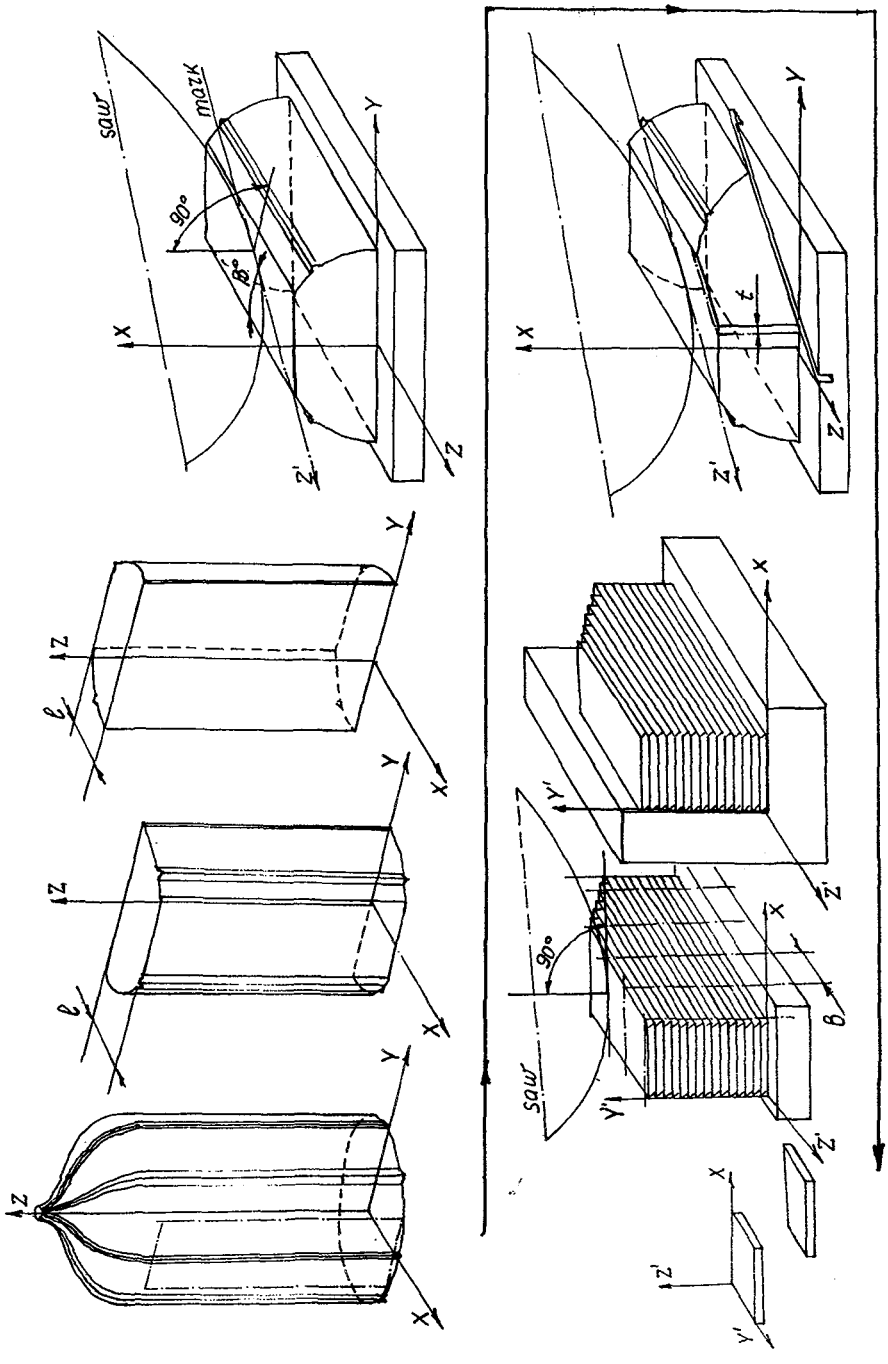

Fig. 4. Technology of cutting LBO crystal boule [001] into yxbl/γ/β plates

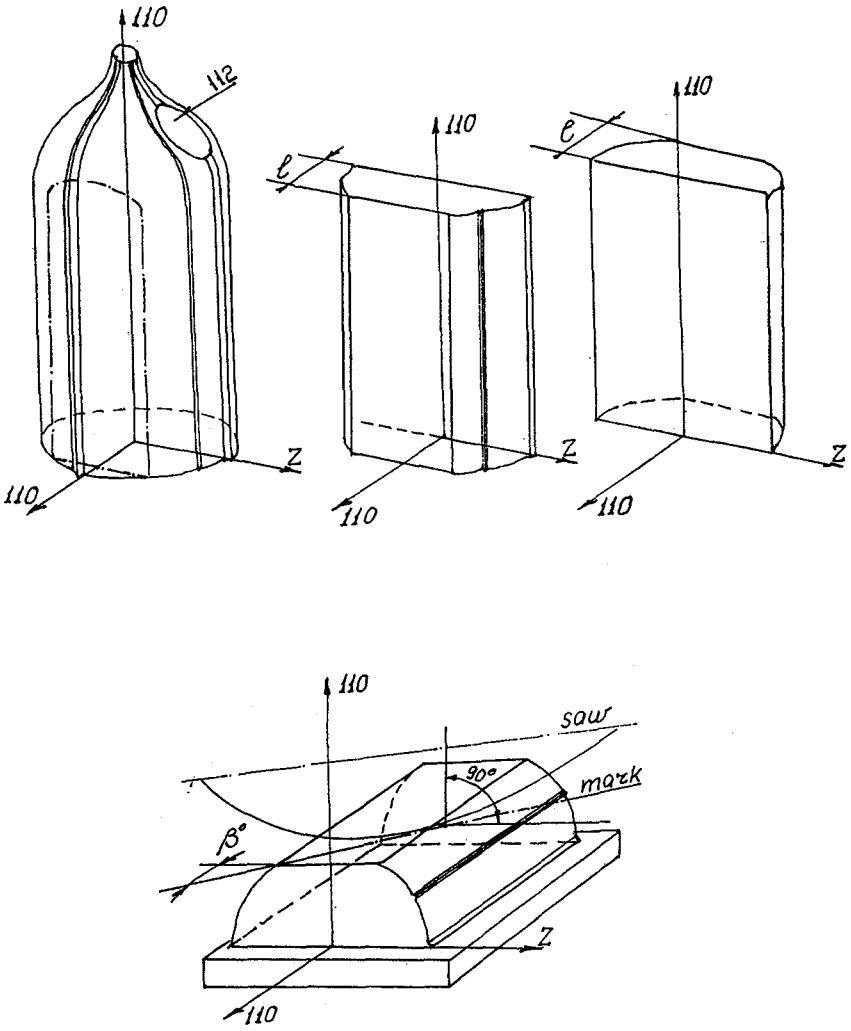

Fig. 5. Technology of cutting LBO crystal boule [110] into yxl/β

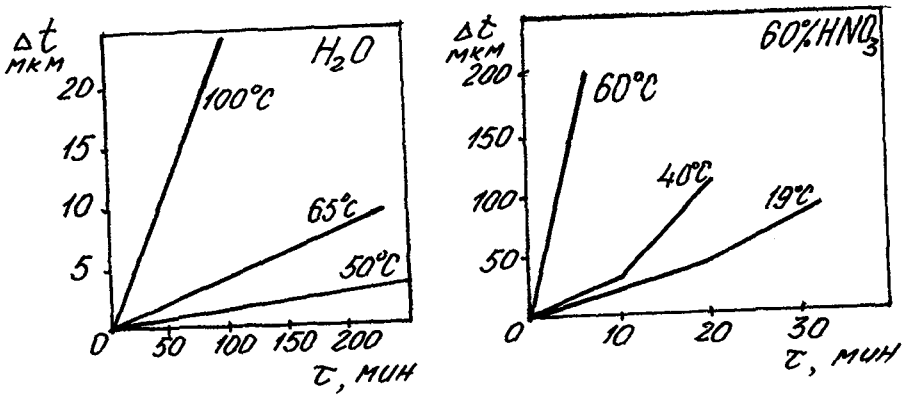

Fig. 6. Kinetic curve of LBO dissolution in hot water and in concentrated HNO_3

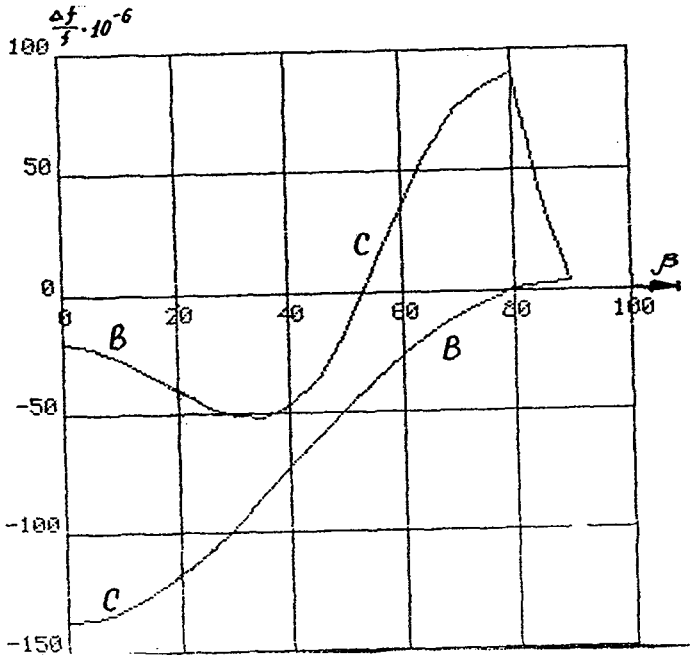

Fig. 7. Dependence of temperature-frequency coefficient of frequency of B and C modes on LBO crystal on the angle of cut YXl/β of a piez.-electric element

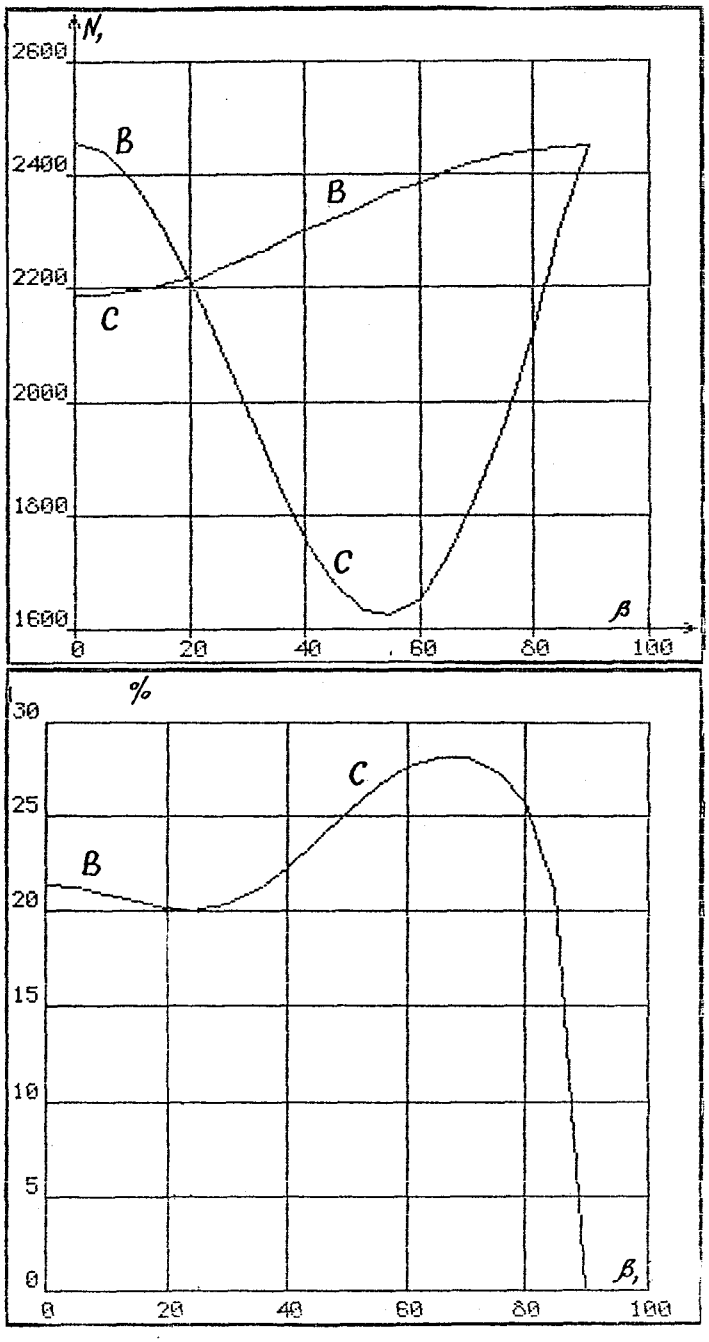

Fig. 8. Dependence of frequency coefficient and electromechanical coupling factor of B- and C-modes in LBO on the angle of cut YXl/β of a piezoelectric element